TO TRAP OR NOT TO TRAP - ANALYZING THE TRADE-OFFS IN DIFFUSION TRANSPORT MODELS

Rushmila Shehreen Khan & Md. Shahriar Karim *
Department of Electrical and Computer Engineering
North South University, Dhaka, Bangladesh
{rushmila.khan.232, shahriar.karim}@northsouth.edu

ABSTRACT

Information transmission by diffusing particles is crucial in many biophysical and artificial systems. The factors that make a diffusive model an optimal choice in a given context remain elusive and vital in narrowing the search space for context-specific applications. This study explores a class of diffusion-reaction paradigms on different performance objectives. Precisely, we compare the robustness, characteristic length scale, and stochastic variability of the competing transport models considering the mesoscopic and microscopic views of the transport, asking whether the entrapment of diffusing molecules improves the reliability of the diffusive transport models.

1 INTRODUCTION

The diffusion transport of particles in short-range signal transmission is critical in many systems, including pattern formation in living species, communication between nanomachines, and target-specific drug delivery mechanisms (Akyildiz et al., 2008; Squires et al., 2008; Wartlick et al., 2009). The spatial presence of particles in these systems results from diffusive transport of various forms; however, the exact details of the underlying mechanism may vary. For instance, amongst the alternative models, the diffusion-decay (DD) model with and without entrapment of diffusing particles is commonly seen in many patterning systems but are of dissimilar spatio-temporal dynamics and characteristics. Specifically, the DD model is pertinent to explain the spatial spread of signaling in many systems, for example, as seen in early embryonic patterning in Drosophila development (Gregor et al., 2007; Bialek & Setayeshgar, 2005). In molecular communications (Pierobon et al., 2014; Kuran et al., 2020; Jamali et al., 2018), a diffusive channel has alternative representations with diffusion of signaling particles as its core (Jamali et al., 2018; 2019; Akyildiz et al., 2008). Other systems, for instance, trap diffusing particles through a series of interactions, affecting dynamics, time-scales, length-scales, efficiency in information transmission, etc (Eldar et al., 2003; Alon, 2019; Umulis et al., 2006). These systems also experience various forms of perturbation, such as variation in production, temperature and pH, viscocity, alterations on the length scale, and the traits also vary between different transport models and in their underlying details (Bialek & Setayeshgar, 2008; Alon, 2019). As in the case of protein movement, the viscocity of the cytoplasm modulates the diffusivity of the particles resulting in an inhomogeneous protein diffusion and regulated activity (Huang et al., 2022). Also, self-enhanced particle degradation provides increased robustness in signaling but at the cost of a reduced characteristic length (Eldar et al., 2003) of the distribution, suggesting further exploration and tuning of contrasting traits between models of dissimilar transport details. Moreover, diffusive transport is a viable model for the formation of potential molecular communication channels (Jamali et al., 2019) that exhibit contrasting traits, necessitating the assessment of alternative diffusion models. Thus, a trade-off between performance objectives in diffusion transport models becomes necessary in many applications and has been the primary focus of our current study.

*Corresponding Author

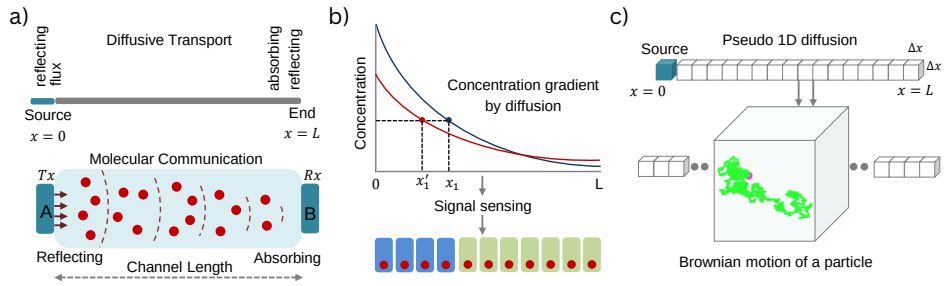

Figure 1: a) Diffusive transport model: Particles emanate from a source and transport away by diffusion in a channel of length L which may relate to envisaged applications such as drug delivery or communications between nanomachines. b) Cellular patterns as a result of morphogen gradient sensing often seen in early embryonic development. c) Pseudo 1D approximation of stochastic transport of a diffusing particle experiencing Brownian motion (approximated by Smoluchowski Equation).

2 Models and Methods

In our preliminary analysis, we consider variants of the three different models representing variations in boundary conditions, source types and degradation mechanisms (Lander et al., 2002). Precisely, the models are subclassed into: i) diffusion-decay (DD) of the diffusive particles that freely diffuse in the medium and undergo degradation at a constant rate (k_δ) and ii) reaction-diffusion (RD) mechanism, where particles in the fluid medium, for instance potential regulators, trap and untrap the diffusing particles, modulating their dynamics. These additional interactions result in an effective diffusivity and degradation rate of the diffusing particles. We also analyze how the strength and the polynomial order of degradation affect the desired performance objectives (Eq. 1 and 3). Such modifications of diffusion dynamics may contribute to a greater advantage in one aspect but with compensation needed in other traits, and have been studied by using deterministic and stochastic models.

2.1 Transport Models: Deterministic View

2.1.1 Diffusion-Degradation: No Trap

$$\frac{\partial C}{\partial t} = D\frac{\partial^2 C}{\partial x^2} - k_\delta \cdot C^m + \text{boundary conditions} + \text{production} + \text{initial condition} \tag{1}$$

In Eq. 1, k_δ is the degradation rate and m denotes the polynomial order of degradation of C. The models include various boundary conditions such as reflecting and flux-boundary, at the left ($x = 0$) and reflecting at the right ($x = L$) end. The source of secretion of the diffusing particle C is assumed to be located at $x = 0$ (see Fig. 1a). At steady state, and with additional simplification, Eq. 1 simplifies to (see Appendix A.1)

$$C(x) = C_0 e^{(-x/\lambda)} \tag{2}$$

where $C_0 = (J\lambda)/D$; J, D, and λ are the flux at $x = 0$, diffusivity of C, and characteristic length scale of diffusing C, respectively.

2.1.2 Reaction-Diffusion: To Trap

$$\frac{\partial C}{\partial t} = D_{C0}\frac{\partial^2 C}{\partial x^2} - k_{\text{on}} C \cdot R + k_{\text{off}} CR, \frac{\partial CR}{\partial t} = D_{CR0}\frac{\partial^2 CR}{\partial x^2} + k_{\text{on}} C \cdot R - (k_{\text{off}} + k_{\text{e}}) \cdot CR$$
$$R_{\text{T}} = R + CR, \text{and Boundary conditions} + \text{production} + \text{initial conditions} \tag{3}$$

Consider that the particles C interact with particles R to form CR, defined as the trapped C. While diffusing away after secretion, the particle C couples and decouples following the first-order and second-order reaction kinetics, respectively. In Eq. 3, k_{on}, k_{off}, and k_{e} are the association, dissociation, and endocytosis rate constants, respectively. R_{T} is the conservation condition on the regulators

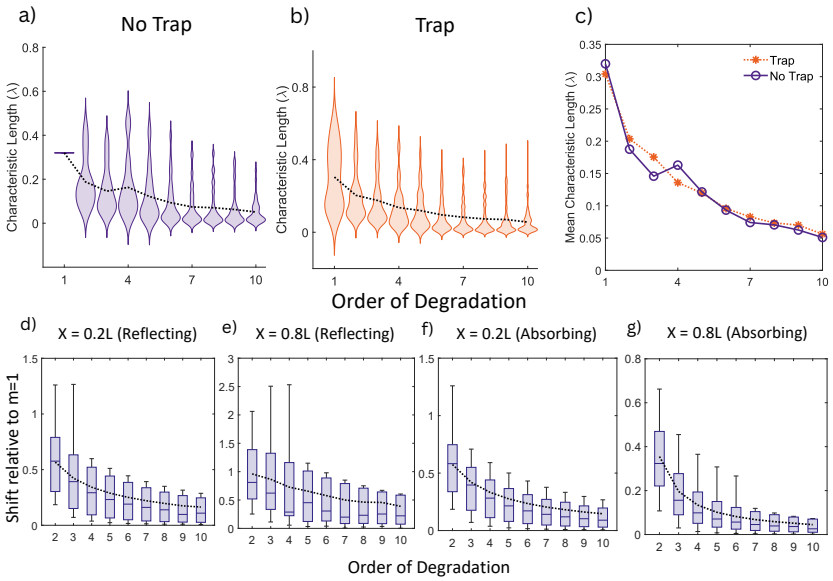

Figure 2: a-c) Mean characteristic length scales of To Trap and No Trap models for selected parameters. d-g) Shift relative to that for linear decay in a No Trap model as we move to higher degree polynomials, for varying D and k_δ at spatial points 20% and 80% of the diffusive length for a reflecting boundary (d,e), 20% and 80% for an absorbing boundary (f,g). Parameters used are provided in A.3

R that trap the diffusing particle C. Assuming that trapped C, denoted as CR, diffuses very slow ($D_{CR0} \approx 0$), and it equilibrates very fast, Eq. 3 simplifies to (see Appendix A.2)

$$\frac{\partial C}{\partial t} = \frac{D_{C0}}{1 + \frac{R_\mathrm{T}}{k_\mathrm{D}}} \frac{\partial^2 C}{\partial x^2} - \frac{k_\mathrm{e} R_\mathrm{T}}{(1 + \frac{R_\mathrm{T}}{k_\mathrm{D}}) k_\mathrm{D}} C = D_\mathrm{eff} \frac{\partial^2 C}{\partial x^2} - k_\mathrm{eff} C \tag{4}$$

As obtained, the entrapment of diffusing particle via a regulator R modifies the diffusivity and degradation of particle C, and appears strikingly similar to Eq. 1. However, entrapment results in an effective diffusivity D_eff and a degradation rate k_eff of the diffusing particle. The numerical simulation of the model in Eq. 3 assumes that the system operates far from saturation, allowing R_T to remain approximately constant spatially.

2.2 Methods

2.2.1 Stochastic Analysis

In stochastic analysis, we implement the diffusive model as in Eq. 1, with and without degradation of C. The model does not consider a flux source, instead, an initial injection of 1000 particles at a position near $x = 0$ at $t = 0$ undergoes Brownian movement with the particles reflected once they hit any of the boundaries on the left ($x = 0$) or right ($x = L$) (see Appendix A.4). Assuming that $X(t) \in \mathbb{R}^1$ represent the position of a diffusing molecule along the x-axis, the particle's Brownian motion is approximated using the stochastic differential equation (Erban et al., 2007; Erban & Chapman, 2009) as

$$X(t + \Delta t) = X(t) + \sqrt{2D\Delta t}\xi_x \tag{5}$$

where D is diffusivity and the $\xi_x \in \mathcal{N}(0, 1)$ represents a normally distributed random number of zero mean and unit variance. Precisely, we perform a stochastic analysis (see Appendix A.4) of 1-D diffusion of particles through Eq. 5, and then further assess it through pseudo-1D assumption, as schematically shown in Fig. 1c.

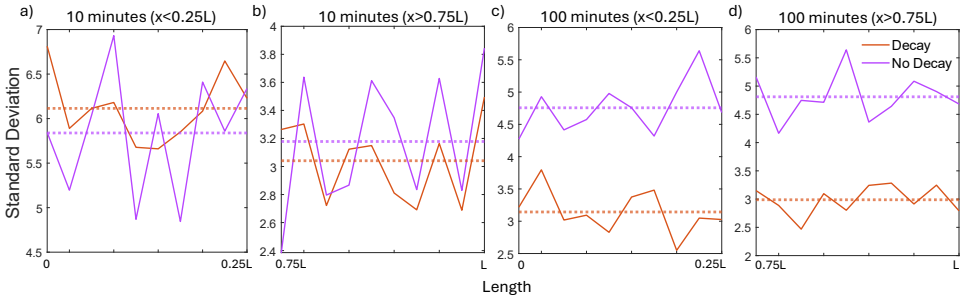

Figure 3: Observation of trends in standard deviation for the stochastic model with and without decay in the immediate region of the source, $L = [0, 10]$ and the sink, $L = [30, 40]$. The dotted line is the mean variation along that region.

2.2.2 METRICS

The model uses robustness and characteristic length scale (λ) as metrics, where λ captures the spatial position x where the concentration of C falls to a level C_0/e (see A.1, Eq. 24). Robustness is defined as the ability of a system to retain its acceptable signaling strength in the presence of perturbations. In this study, we perturb the production J of the signaling particle and assess the positional shift (Fig. 2) defined as

$$S_J = (S_{x1}, S_{x2}, \dots S_{xn})/S_J^{\max}, \text{where}, S_J^{\max} = \max(S_{x1}, S_{x2}, \dots S_{xn})$$
$$S_{2J} = (S_{x1}, S_{x2}, \dots S_{xn})/S_J^{\max} \tag{6}$$

The positional shift is calculated as $\Delta x = |x_1 - x_1^{'}|$. Here, we take a concentration (S_{x1}) from S_J at position x_1, and look for this same concentration in S_{2J}. The position where S_{x1} appears in S_{2J} is $x_1^{'}$. A low magnitude of Δx relates to better robustness demonstrated by the system.

3 RESULTS

In the No Trap models (Eq. 1), we varied the degradation mechanism to capture the positional change at $x = 0.2$ and $x = 0.8$ for the perturbations of the flux (J) of C and varied intrinsic diffusivity and other parameters over a parameter space (Fig. 2d-g). As seen, the No Trap model achieves improved robustness (measured by definition in Eq. 6) for higher-order polynomial degradation (denoted using m in Eq. 1), as demonstrated in earlier studies (Eldar et al., 2003). However, the improvement saturates after m reaches a particular maximum order beyond which the polynomial-order degradation does not achieve much. Specifically, robustness improves negligibly, and the added benefits of higher order polynomial degradation of C become indistinguishable. Furthermore, many patterning systems need an extended spatial presence of the particles (Alon, 2019) in addition to enhanced robustness against perturbations. Here, we capture the spatial presence of particles using the characteristic length scale λ as the metric, as in Fig. 2a, where λ gradually decreases with an increase in the order (m) of degradation. A comparison between the No Trap and To Trap model reveals a superior performance for the To Trap model, showing an increased λ (Figure. 2) for $m = 2, 3$. The study was conducted over large parameter space covering several order of magnitudes of parameters (see Table. 2, Appendix) affecting the model dynamics. Interestingly, self-enhanced degradation model ($m = 2$) also suggests improved robustness (Eldar et al., 2003), indicating its relevance from multiobjective necessity. For the parameter sets (No Trap: 511, and To Trap: 5281) that produce acceptable distributions (see Figure. 5, Appendix) of diffusing particles C, λ is smaller for a degradation order $m > 1$, suggesting strong kinetic dependency of higher λ. One immediate analysis we continue is identifying the required conditions for higher order degradation that achieve a greater λ value. Aside from this, an initial comparison between the To Trap and No Trap model suggests that if particles are trapped while diffusing, the system may appear more robust than a model that avoids trapping diffusing particles, with comparable λ for the To Trap model (see Appendix, Figure. 4). Together, the initial study reports that the trapping of particles absorbs perturbations better with insignificant advantages for higher order ($m > 4$) degradations; however, additional study of tuning and screening of the models' dynamics is necessary to substantiate further.

In stochastic analysis, initially we compare the role of free diffusion and the diffusion-decay phenomenon by simulating exact Brownian dynamics of the diffusing particles C. Here, we calculate standard deviation (σ) around the mean level of C over $n = 50$ runs at $t_1 = 10$ and $t_2 = 100$ minutes for each spatial position. An interesting phenomenon emerges showing region specific dynamic behavior of σ. Specifically, mean level of σ calculated for $x \leq 0.25L$ for free diffusion model is smaller than DD model, which, however, gets altered in region ($x > 0.75L$ and $x \leq L$) when computed at $t_1 = 10$ minutes (Figure. 3a-b). However, DD model exhibits less standard deviation (See Figure. 3c-d) for both $x \leq 0.25L$ and ($x > 0.75L$ and $x \leq L$) if the dynamics evolve for a longer duration ($t_2 = 100$ min). Here, the mean of standard deviation in regions up to $0.25L$ and beyond $0.75L$ dynamically alter for short-term dynamics and remain uniform for long-term dynamics, indicating the necessity of an extended analysis of different dynamic traits and precision in competing transport models. Precisely, in many situations, information transmission or downstream activation of signaling by a diffusive transport may trigger at the pre-steady state (Alon, 2019) and may be affected by the alterations observed in this study. Also, such dynamic difference of standard deviation may be relevant to mandatory traits such as dynamic scaling necessary by pattern formation systems (Umulis, 2009).

4 Discussion

We started the proposed work by interrogating the fundamental question of the nature, type, or context of optimal diffusive transport models seen in living species. Our preliminary analysis demonstrates that models perform differently depending on whether particles degrade while diffusing. The type of degradation also matters when it comes to robustness and length-scale adjustment for different applications. Interestingly, performance objectives are kinetic-dependent, vary in exact molecular details, and appear qualitatively different under alternative boundary conditions, making a wide range of model possibilities. An immediate caveat of the current study is its lack of a detailed microscopic analysis that involves mutual information, channel capacity, etc., which becomes essential, and so does the first-passage time (Van Kampen, 1992). Also, simulation assumptions should be relaxed and alternative boundary conditions on the particles' secretion must be studied extensively (Erban & Chapman, 2007). Together, these findings are vital for strengthening our understanding of the intricate details of diffusive transport that occurs in a living cell. These observations may be relevant to the AI Virtual Cell (AIVC) (Bunne et al., 2024) initiative undertaken to design and develop a neural network-based framework that represents the simulated behavior of a living cell, for example, the movement of proteins, diffusion of RNA in cytoplasmic regions (Chen et al., 2014). As conceptualized, the AIVC must capture a multiscale universal representation that should integrate molecular and cellular interactions and information processing across different scales. Cell processes change due to numerous extrinsic and intrinsic factors, and narrowing the search space for biologically feasible information integration at the molecular, cellular, and multicellular scale is crucial to obtaining the high-quality training data necessary for AIVC implementation. Overall, whether a particle is to be trapped or not to be trapped requires additional model exploration, including the inhibitor model both on a mesoscopic and microscopic scale, to shed light on the underlying reasons behind evolutionary choices made in many living systems and has been a part of our ongoing research.

References

Ian F Akyildiz, Fernando Brunetti, and Cristina Blázquez. Nanonetworks: A new communication paradigm. *Computer Networks*, 52(12):2260–2279, 2008.

Uri Alon. *An introduction to systems biology: design principles of biological circuits*. Chapman and Hall/CRC, 2019.

William Bialek and Sima Setayeshgar. Physical limits to biochemical signaling. *Proceedings of the National Academy of Sciences*, 102(29):10040–10045, 2005.

William Bialek and Sima Setayeshgar. Cooperativity, sensitivity, and noise in biochemical signaling. *Physical Review Letters*, 100(25):258101, 2008.

Charlotte Bunne, Yusuf Roohani, Yanay Rosen, Ankit Gupta, Xikun Zhang, Marcel Roed, Theo Alexandrov, Mohammed AlQuraishi, Patricia Brennan, Daniel B Burkhardt, et al. How to build

the virtual cell with artificial intelligence: Priorities and opportunities. *Cell*, 187(25):7045–7063, 2024.

Jianbo Chen, David Grunwald, Luca Sardo, Andrea Galli, Sergey Plisov, Olga A Nikolaitchik, De Chen, Stephen Lockett, Daniel R Larson, Vinay K Pathak, et al. Cytoplasmic hiv-1 rna is mainly transported by diffusion in the presence or absence of gag protein. *Proceedings of the National Academy of Sciences*, 111(48):E5205–E5213, 2014.

Avigdor Eldar, Dalia Rosin, Ben-Zion Shilo, and Naama Barkai. Self-enhanced ligand degradation underlies robustness of morphogen gradients. *Developmental cell*, 5(4):635–646, 2003.

Radek Erban and S Jonathan Chapman. Reactive boundary conditions for stochastic simulations of reaction–diffusion processes. *Physical Biology*, 4(1):16, 2007.

Radek Erban and S Jonathan Chapman. Stochastic modelling of reaction–diffusion processes: algorithms for bimolecular reactions. *Physical biology*, 6(4):046001, 2009.

Radek Erban, Jonathan Chapman, and Philip Maini. A practical guide to stochastic simulations of reaction-diffusion processes. *arXiv preprint arXiv:0704.1908*, 2007.

Thomas Gregor, Eric F Wieschaus, Alistair P McGregor, William Bialek, and David W Tank. Stability and nuclear dynamics of the bicoid morphogen gradient. *Cell*, 130(1):141–152, 2007.

William YC Huang, Xianrui Cheng, and James E Ferrell Jr. Cytoplasmic organization promotes protein diffusion in xenopus extracts. *Nature Communications*, 13(1):5599, 2022.

Vahid Jamali, Nariman Farsad, Robert Schober, and Andrea Goldsmith. Diffusive molecular communications with reactive molecules: Channel modeling and signal design. *IEEE Transactions on Molecular, Biological, and Multi-Scale Communications*, 4(3):171–188, 2018.

Vahid Jamali, Arman Ahmadzadeh, Wayan Wicke, Adam Noel, and Robert Schober. Channel modeling for diffusive molecular communication—a tutorial review. *Proceedings of the IEEE*, 107 (7):1256–1301, 2019.

Mehmet Şükrü Kuran, H Birkan Yilmaz, Ilker Demirkol, Nariman Farsad, and Andrea Goldsmith. A survey on modulation techniques in molecular communication via diffusion. *IEEE Communications Surveys & Tutorials*, 23(1):7–28, 2020.

Arthur D Lander, Qing Nie, and Frederic YM Wan. Do morphogen gradients arise by diffusion? *Developmental cell*, 2(6):785–796, 2002.

Massimiliano Pierobon, Ian F Akyildiz, et al. Fundamentals of diffusion-based molecular communication in nanonetworks. *Foundations and Trends® in Networking*, 8(1-2):1–147, 2014.

Todd M Squires, Robert J Messinger, and Scott R Manalis. Making it stick: convection, reaction and diffusion in surface-based biosensors. *Nature biotechnology*, 26(4):417–426, 2008.

David M Umulis. Analysis of dynamic morphogen scale invariance. *Journal of The Royal Society Interface*, 6(41):1179–1191, 2009.

David M Umulis, Mihaela Serpe, Michael B O'Connor, and Hans G Othmer. Robust, bistable patterning of the dorsal surface of the drosophila embryo. *Proceedings of the National Academy of Sciences*, 103(31):11613–11618, 2006.

Nicolaas Godfried Van Kampen. *Stochastic processes in physics and chemistry*, volume 1. Elsevier, 1992.

Ortrud Wartlick, Anna Kicheva, and Marcos González-Gaitán. Morphogen gradient formation. *Cold Spring Harbor perspectives in biology*, 1(3):a001255, 2009.

A APPENDIX

A.1 NO TRAP MODELS

A.1.1 FLUX AT SOURCE

We consider the following diffusion equation and the tabulated initial and boundary conditions,

$$\frac{\partial C}{\partial t} = D\frac{\partial^2 C}{\partial x^2} - k_\delta C^m, m = 1, 2, \ldots, n$$

Initial Condition	Left Boundary	Right Boundary
$C(x, 0) = 0$	$-D\frac{\partial C}{\partial x} = J$	Reflecting: $\frac{\partial C}{\partial x} = 0$
-do-	-do-	Absorbing: $C(L, t) = 0$

Table 1: Initial and Boundary conditions: No Trap (flux at source)

We use a central difference scheme to discretize the PDEs.

$$\frac{\partial^2 C}{\partial x^2} = \frac{C_{i-1} - 2C_i + C_{i+1}}{\Delta x^2} \quad (7) \qquad \frac{\partial C}{\partial x} = \frac{C_{i+1} - C_{i-1}}{2\Delta x} \quad (8)$$

Using equation 7 and equation 8, we find the expressions for artificial nodes at the reflecting left and right boundaries:

$$C_{-1} = C_1 + \frac{J}{D}2\Delta x \quad (9) \qquad C_{L+1} = C_{L-1} \quad (10)$$

Hence, we have the following systems of ODEs.

1. Right Boundary Reflecting

$$\frac{\partial C(i,t)}{\partial t} = \begin{cases} D(\frac{2C_1 + \frac{J}{D}2\Delta x - 2C_0}{\Delta x^2}) - k_\delta C_0^m, m = 1, 2 & , i = 0 \\ D\frac{C_{i-1} - 2C_i + C_{i+1}}{\Delta x^2} - k_\delta C_i^m, m = 1, 2 & , 1 \leq i \leq N - 1 \\ D(\frac{2C_{L-1} - 2C_L}{\Delta x^2}), -k_\delta C_L^m, m = 1, 2 & , i = N \end{cases} \quad (11)$$

2. Right Boundary Absorbing

$$\frac{\partial C(i,t)}{\partial t} = \begin{cases} D(\frac{2C_1 + \frac{J}{D}2\Delta x - 2C_0}{\Delta x^2}) - k_\delta C_0^m, m = 1, 2 & , i = 0 \\ D\frac{C_{i-1} - 2C_i + C_{i+1}}{\Delta x^2} - k_\delta C_i^m, m = 1, 2 & , 1 \leq i \leq N - 1 \end{cases} \quad (12)$$

A.1.2 CHARACTERISTIC LENGTH OF NO TRAP MODEL WITH REFLECTING BOUNDARIES

$$\frac{\partial C}{\partial t} = D\frac{\partial^2 C}{\partial x^2} - kC, D\frac{\partial C}{\partial x}\bigg|_{x=0} = -J, \frac{\partial C}{\partial x}\bigg|_{x=L} = 0$$

At steady state, we have

$$D\frac{\partial^2 C}{\partial x^2} - kC = 0$$
$$\frac{\partial^2 C}{\partial x^2} = \frac{kC}{D} = C_0\frac{1}{\lambda^2}$$

From this, we know

$$\lambda = \sqrt{\frac{D}{k}}$$

The generic solution is,

$$C = C_0 e^{-\frac{x}{\lambda}} + C_1 e^{\frac{x}{\lambda}}$$

We use the boundary conditions to find the values of C_0 and C_1.

$$\frac{\partial C}{\partial x} = \frac{\partial}{\partial x}(C_0 e^{-\frac{x}{\lambda}} + C_1 e^{\frac{x}{\lambda}}) = -\frac{1}{\lambda} C_0 e^{-\frac{x}{\lambda}} + \frac{1}{\lambda} C_1 e^{\frac{x}{\lambda}} \tag{13}$$

Taking the derivative of equation 13:

$$\frac{\partial^2 C}{\partial x^2} = \frac{C_1 e^{\frac{x}{\lambda}}}{\lambda^2} + \frac{C_0 e^{-\frac{x}{\lambda}}}{\lambda^2} \tag{14}$$

Now, we apply the right boundary condition.

$$\left.\frac{\partial C}{\partial x}\right|_{x=L} = -\frac{1}{\lambda} C_0 e^{-\frac{L}{\lambda}} + \frac{1}{\lambda} C_1 e^{\frac{L}{\lambda}} = 0 \Rightarrow C_1 = C_0 e^{-\frac{2L}{\lambda}} \tag{15}$$

Applying the left boundary condition,

$$\left.\frac{\partial C}{\partial x}\right|_{x=0} = -\frac{J}{D} \Rightarrow C_1 - C_0 = -\frac{J\lambda}{D} \tag{16}$$

Substituting equation 15 in equation 16,

$$C_0 e^{-\frac{2L}{\lambda}} - C_0 = -\frac{J\lambda}{D} \Rightarrow C_0 = \frac{J\lambda}{D(1 - e^{-\frac{2L}{\lambda}})} \tag{17}$$

Following from equation 17

$$C_1 = \frac{J\lambda(e^{-\frac{2L}{\lambda}})}{D(1 - e^{-\frac{2L}{\lambda}})} \tag{18}$$

Substituting equation 17 and equation 18 into the generic solution we get,

$$C(x) = C_0 e^{-\frac{x}{\lambda}} + C_1 e^{\frac{x}{\lambda}} = \frac{J\lambda}{D(1 - e^{-\frac{2L}{\lambda}})}(e^{-\frac{x}{\lambda}} + e^{-\frac{2L}{\lambda} + \frac{x}{\lambda}}) \tag{19}$$

As $L \gg \lambda$, we have the expression

$$C(x) = \frac{J\lambda}{D}(e^{-\frac{x}{\lambda}}) \tag{20}$$

Applying $L \gg \lambda$ to equation 17 and equation 18, we get

$$C_0 = \frac{J\lambda}{D} \quad (21) \qquad\qquad C_1 = 0 \quad (22)$$

Combining equation 21 with $\lambda = \sqrt{\frac{D}{k}}$,

$$C(x) = C_0 e^{-\frac{x}{\lambda}} \tag{23}$$

Dimensional analysis of λ gives us the following:

$$\lambda = \sqrt{\frac{D}{k}} = \sqrt{\frac{[L^2 T^{-1}]}{[T^{-1}]}} = [L]$$

Finally, we have an expression for the concentration at the characteristic length of a diffusive model,

$$\left.C(x)\right|_{x=\lambda} = \frac{C_0}{e} \tag{24}$$

A.2 To Trap Model

We consider the following diffusion model with a trapping mechanism, which has the corresponding boundary conditions.

$$\frac{\partial C}{\partial t} = D_{C0}\frac{\partial^2 C}{\partial x^2} - k_{\text{on}}C \cdot R + k_{\text{off}}CR, \frac{\partial CR}{\partial t} = D_{CR0}\frac{\partial^2 CR}{\partial x^2} + k_{\text{on}}C \cdot R - k_{\text{off}}CR - k_{\text{e}}CR,$$
$$R_{\text{T}} = R + CR, \left.\frac{\partial C}{\partial x}\right|_{x=0} = -\frac{J}{D_{C0}}, \left.\frac{\partial C}{\partial x}\right|_{x=L} = 0$$

In this model, k_{on} is the forward reaction rate constant, k_{off} is the backward reaction rate constant, and k_{e} is the endocytosis rate. R is a regulator, CR is the bounded particle and R_{T} is the conservation condition. Assuming D_{CR0} is very low, we have the following.

$$\frac{\partial CR}{\partial t} = k_{\text{on}}C \cdot R - CR(k_{\text{off}} + k_{\text{e}})$$

Further, assuming $\frac{\partial CR}{\partial t} = 0$, we get

$$CR = \frac{k_{\text{on}}}{k_{\text{off}} + k_{\text{e}}}(C \cdot R) = \frac{C(R_{\text{T}} - CR)}{\frac{k_{\text{off}}+k_{\text{e}}}{k_{\text{on}}}} = \frac{C(R_{\text{T}} - CR)}{k_{\text{D}}} = \frac{C \cdot R_{\text{T}}}{C + k_{\text{D}}}$$

When $k_{\text{D}} \gg C$,

$$CR \approx \frac{C \cdot R_{\text{T}}}{k_{\text{D}}} \tag{25}$$

Adding $\frac{\partial C}{\partial t}$ and $\frac{\partial CR}{\partial t}$,

$$\frac{\partial C}{\partial t} + \frac{\partial CR}{\partial t} = D_{C0}\frac{\partial^2 C}{\partial x^2} - k_{\text{e}}CR \tag{26}$$

Substituting equation 25 in equation 26,

$$\begin{aligned} \frac{\partial C}{\partial t}(1 + \frac{R_{\text{T}}}{k_{\text{D}}}) &= D_{C0}\frac{\partial^2 C}{\partial x^2} - k_{\text{e}}(\frac{C \cdot R_{\text{T}}}{k_{\text{D}}}) \\ \frac{\partial C}{\partial t} &= \frac{D_{C0}}{1 + \frac{R_{\text{T}}}{k_{\text{D}}}}\frac{\partial^2 C}{\partial x^2} - \frac{k_{\text{e}}R_{\text{T}}}{(1 + \frac{R_{\text{T}}}{k_{\text{D}}})k_{\text{D}}}C = D_{\text{eff}}\frac{\partial^2 C}{\partial x^2} - k_{\text{eff}}C \end{aligned} \tag{27}$$

where D_{eff} and k_{eff} are the effective diffusion coefficient and the effective degradation rate. Following the derivation done for the No Trap model, we have $\lambda = \sqrt{\frac{D_{\text{eff}}}{k_{\text{eff}}}}$, and from equation 21,

$$C_0 = \frac{J\lambda}{D_{C0}} \tag{28}$$

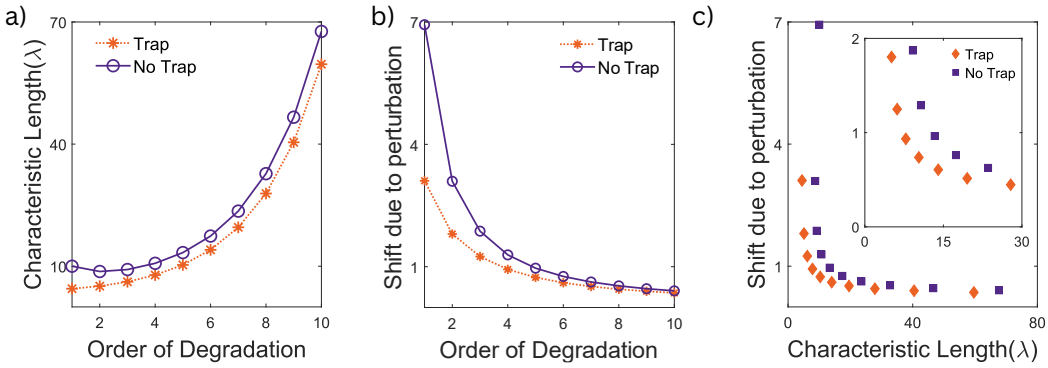

Figure 4: Characteristic length and shift comparison for the Trap and No Trap models, $L = 500\mu m$.

A.3 PARAMETERS

Parameter	Value	Unit
D	[0.00001, 0.0001, 0.001, 0.01, 0.1, 1, 10]	$\mu m^{-2}s^{-1}$
D_{c_0}	[0.00001, 0.0001, 0.001, 0.01, 0.1, 1, 10]	$\mu m^{-2}s^{-1}$
k	[0.00001, 0.0001, 0.001, 0.01, 0.1, 1, 10]	s^{-1}
k_{on}	[0.0001, 0.001, 0.1, 1]	$nM^{-1}s^{-1}$
k_{off}	[0.01, 1, 1.5, 2.5]	s^{-1}
k_{e}	[0.01, 1, 1.5, 2.5]	s^{-1}
R_{T}	10	nM
J	[0.05 0.1 0.5 1 5]	$nM\mu m^{-2}s^{-1}$

Table 2: Parameter set used for screening gradients. The filtered out combinations were used in the Trap and No Trap Models in Fig. 2 a-c.

Parameter	Value	Unit
D	[0.01, 0.1, 1]	$\mu m^{-2}s^{-1}$
k	[0.0001, 0.001, 0.01, 0.1]	s^{-1}
J (Unperturbed)	0.05	$nM\mu m^{-2}s^{-1}$
J (Perturbed)	0.1	$nM\mu m^{-2}s^{-1}$

Table 3: Parameter set used in the No Trap models for robustness analysis in Fig. 2 d-g.

Parameter	Value	Unit
D	0.1	$\mu m^{-2}s^{-1}$
D_{c_0}	0.1	$\mu m^{-2}s^{-1}$
k	0.001	s^{-1}
k_{on}	0.001	$nM^{-1}s^{-1}$
k_{off}	1.5	s^{-1}
k_{e}	1.5	s^{-1}
R_{T}	10	nM
J (Unperturbed)	0.05	$nM\mu m^{-2}s^{-1}$
J (Perturbed)	0.1	$nM\mu m^{-2}s^{-1}$

Table 4: Parameters used in the Trap and No Trap Models in Fig. 4

Parameter	Value	Unit
D	0.01	$\mu m^{-2}s^{-1}$
D_{c_0}	0.1	$\mu m^{-2}s^{-1}$
k	0.00001	s^{-1}
k_{on}	0.0001	$nM^{-1}s^{-1}$
k_{off}	0.01	s^{-1}
k_{e}	0.01	s^{-1}
R_{T}	10	nM
J (Trap)	0.05	$nM\mu m^{-2}s^{-1}$
J (No Trap)	0.05	$nM\mu m^{-2}s^{-1}$

Table 5: Parameters used in the acceptable gradients in Fig. 5 with linear degradation.

Parameter	Value	Unit
D	0.01	$\mu m^{-2}s^{-1}$
D_{c_0}	0.0001	$\mu m^{-2}s^{-1}$
k	0.01	s^{-1}
k_{on}	0.0001	$nM^{-1}s^{-1}$
k_{off}	0.01	s^{-1}
k_{e}	0.01	s^{-1}
R_{T}	10	nM
J (Trap)	0.1	$nM\mu m^{-2}s^{-1}$
J (No Trap)	0.05	$nM\mu m^{-2}s^{-1}$

Table 6: Parameters used in the unacceptable gradients in Fig. 5 with linear degradation.

Parameters were screened in two phases. Firstly, parameter combinations for which the discretized steady-state solution did not align with its analytical counterpart, were removed. The combinations of D, k and J which carried over, were used to compute discretized solutions for polynomial order degradation up to $m = 10$.

From all the resulting steady-state solutions, we picked out the concentration gradients where C at $x = 0.25L$ is at least $0.1C_{max}$ and C at $x = L$ is less than $0.3C_{max}$. A comparison of acceptable and unacceptable gradients is given in Figure 5.

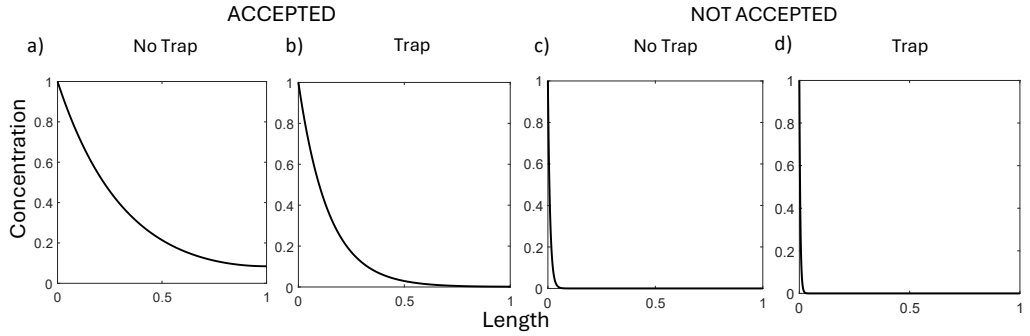

Figure 5: A comparison of acceptable (a,b) and unacceptable (c,d) gradients.

A.4 STOCHASTIC SIMULATION STEPS

The Smolochowski equations for Brownian dynamics consider the following steps (Erban et al., 2007; Erban & Chapman, 2009):

(a) Generated $\xi \in \mathcal{N}(0, 1)$

(b) Calculated the position of all 1000 particles injected at x = 0 and t = 0 using $X(t + \Delta t) = X(t) + \sqrt{2D\Delta t}\xi$

(c) if $X(t + \Delta t)$ of a partile is < 0, we replace $X(t + \Delta t) = -X(t) - \sqrt{2D\Delta t}\xi$ and it takes care of the particles crossing the left boundary at $x = 0$.

(d) if $X(t + \Delta t)$ of a partile is $> L$, we replace $X(t + \Delta t) = 2L - X(t) - \sqrt{2D\Delta t}\xi$, and takes care of the particles that cross the right boundary at $x = L$.

(e) Steps (c) and (d) mimic the reflecting boundary conditions at both ends.

For the degradation of the particles undergoing Brownian dynamics, the following step is considered

(a) **Degradation:** For sufficiently small Δt, the term $k_1 \Delta t_1 \leq 1$ denotes the probability that a particle is degraded between $[t, t + \Delta t)$. To remove a particle from the system due to degradation, we generate a uniform $(0, 1)$ random variable r. If $c(t)k\Delta t > r$, then a particle is removed from the system. That is, $c(t + \Delta t) = c(t) - 1$.